589-nm yellow laser generation by intra-cavity sum-frequency mixing in a T-shaped Nd:YAG laser cavity

Xiuyan Chen (陈秀艳)[1,2], Xiu Li (李 修)[1,2], Haolei Zhang (张豪磊)[1,2], Haowei Chen (陈浩伟)[2,3], Jintao Bai (白晋涛)[1,2,3], and Zhaoyu Ren (任兆玉)[1,2*]

[1] *Institute of Photonics and Photo-Technology, Provincial Key Laboratory of Photoelectronic Technology, Northwest University, Xi'an 710069, China*

[2] *Shaanxi Engineering Technology Research Center for Solid State Lasers and Application, Northwest University, Xi' an 710069, China*

[3] *Department of Physics, Northwest University, Xi'an 710069, China*

[*] *E-mail: rzynwu@yahoo.cn*

Received December 25, 2008

To obtain high power 589-nm yellow laser, a T-shaped thermal-insensitive cavity is designed. The optimal power ratio of 1064- and 1319-nm beams is considered and the fundamental spot size distribution from the output mirror to the two laser rods are calculated and simulated, respectively. As a result, a 589-nm yellow laser with the average output power of 5.7 W is obtained in the experiment when the total pumping power is 695 W. The optical-to-optical conversion efficiency from the fundamental waves to the sum frequency generation is about 15.2% and the pulse width is 150 ns at the repetition rate of 18 kHz. The instability of the yellow laser is also measured, which is less than 2% within 3 h. The beam quality factors are $M_x^2 = 4.96$ and $M_y^2 = 5.08$.

OCIS codes: 140.0140, 190.0190.

doi: 10.3788/COL20090709.0815.

Nowadays, all-solid-state lasers have become a hot research topic in the laser industry because of the advantages of compactness, robustness, high efficiency, good beam quality, environment protection, and so on[1−4]. Especially, after the nonlinear optical frequency conversion technology and laser diode (LD) technique were combined, various solid-state lasers (red, blue, and ultraviolet, etc.) were developed rapidly and widely, and lots of papers reported the products and their applications. It is a pity that the coherent radiations in the range of 560−650 nm have not been obtained by frequency doubling owing to the absence of corresponding fundamental beams emitted from the laser crystals. However, the yellow laser at 589 nm is of unique value and application in many fields, such as bio-medical research, laser display, Bose-Einstein condensation, astronomical observation, military industry, etc., therefore many researchers put their heart into developing solid-state yellow lasers so as to satisfy different requirements[5−10].

In the 1990s, when the solid-state yellow laser was still in its initial stage, a single Nd:YAG crystal, which emits 1064- and 1319-nm radiations simultaneously, was usually adopted in the laser system[11−13]. However, that method requires high coating technique and has the disadvantages of low output power and poor light beam quality, which limits the application of yellow lasers in certain area. So in this century, two and more gain media, along with mode locking and optical amplification technologies, are introduced into the generation device of 589-nm yellow lasers[14,15]. As a result, the output power of yellow lasers using these kinds of schemes is very high, which could be up to 50 W, but the configurations are complex, the resonators are too long, and the nonlinear crystals are generally used in the external cavity.

In this letter, a T-shaped thermal-insensitive cavity is designed to obtain high power 589-nm yellow laser by intra-cavity sum-frequency mixing. A 45° coupling mirror is adopted, which determines the polarizations of the two fundamental beams and couples them coaxially into the KTP crystal for sum-frequency generation. On the basis of calculating and simulating the cavity stability versus the thermal focal length of the two laser rods and the fundamental spot size distribution from the output coupler to two rods, a 5.7-W 589-nm yellow laser is obtained in the experiment when the total pumping power is 695 W. At the maximum output power, the optical-to-optical conversion efficiency from the fundamental waves to the sum frequency generation is 15.2%. The pulse width of 150 ns at the repetition rate of 18 kHz and the instability of 2% within 3 h are also measured.

The experimental setup for intra-cavity sum-frequency mixing is illustrated in Fig. 1. The 1064-nm coherent light oscillates in the linear cavity made up of the mirrors M_1 and M_3, and the 1319-nm laser oscillates in the L-shaped cavity composed of the mirrors M_2, M_4, and M_3. The end mirrors M_1 and M_2 are both plano-concave mirrors with the same radius of 100 cm and the concave surfaces are coated with high reflectance (HR) at 1064 and 1319 nm, respectively. The others are plane mirrors. For the output coupler M_3, one surface has both dual-wavelength HR at 1064 and 1319 nm and high transmittance (HT) at 589 nm, and the other surface is coated with anti-reflectance (AR) at 589 nm to extract the yellow beam from the resonator. The mirror M_4 is placed in the laser system at an angle of 45° to the horizontal direction. Both the surfaces S_1 and S_2 are coated with HT for 1064-nm laser in horizontal (p-polarized) direction, and the surface S_2 is also coated with HR for 1319-nm laser

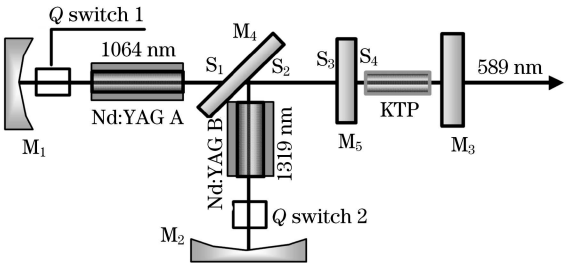

Fig. 1. Schematic of the cavity configuration.

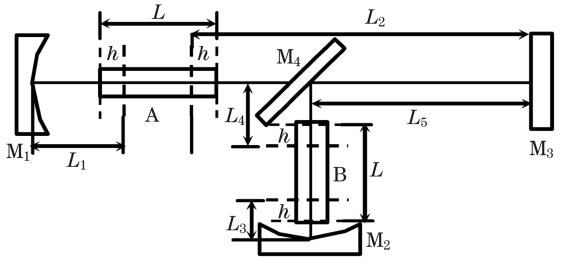

Fig. 2. Corresponding lens-like equivalent resonator.

in vertical (s-polarized) direction. The mirror M_5 serves as a harmonic reflector and prevents the yellow laser from entering into the gain media so as to reduce the waste heat generation. Both the surfaces S_3 and S_4 have dual-wavelength HT coatings at 1064 and 1319 nm, and S_4 has also HR coating at 589 nm. The two laser modules with the same geometry are employed, and each one consists of thirty 20-W LDs and a Nd:YAG rod (Φ4.0×90 (mm), Nd^{3+}-doping concentration of 0.8 at.-%). The Nd:YAG rod A is coated with AR film at 1064 nm on the two end faces, and the Nd:YAG rod B is coated with HT coatings at both 1064 and 1319 nm. In addition, two acousto-optic modulators (AOMs) are placed near the two rods respectively to achieve higher diffraction loss, which is beneficial to nonlinear frequency conversion. A KTP crystal cut for type-II critical phase matching is employed as the intra-cavity sum-frequency crystal between the mirrors M_5 and M_3. Both the surfaces are coated with AR coatings at 1064, 1319, and 589 nm to reduce intra-cavity reflection losses. The temperature of the KTP crystal is kept constant for decreasing the thermal lens effect, compensating for the phase mismatching, and improving the frequency conversion efficiency.

It is well known that thermal lens effect of the gain medium must be considered in the resonator system design because it will influence the laser performance in many aspects[16,17]. On the one hand, thermal lens effect is the main factor that affects the cavity stability, and it will become more and more obvious with the increase of pumping power because the thermal focal length can change from infinite to several tens of centimeters. When the laser system operates in the stable region, the output power of the coherent light will increase with the improvement of pumping power. When it works in the unstable region, the output power will decrease with the increase of pumping power. Therefore, it is quite necessary to design a thermal-insensitive cavity running in a wide region of pumping power to obtain high power of yellow laser. On the other hand, thermal lens effect of the gain medium is also related to the fundamental spot size in the resonator, which will affect laser beam quality and nonlinear frequency conversion efficiency, so analyzing the relationship mentioned above is of instructive significance for the experiment.

In general, the laser rod can be equivalent to a lens-like medium under the high power pumping condition, and this simplification has been applied widely. The distance between the principal plane and the nearest end of the rod is $h = L/2n$, where L is the geometric length of the rod and n is the refraction index[18]. The schematic drawing of the cavity configuration in the experiment and its lens-like equivalent resonator are shown in Figs. 1 and 2, respectively.

Assuming that the thermal focal length of rods A and B are f_1 and f_2 respectively, the mirror M_1 is a reference plane for the 1064-nm resonator and M_2 for the 1319-nm resonator, and the round-trip $ABCD$ matrix for the linear and L-shaped cavities can be described as

$$\begin{bmatrix} A_1 & B_1 \\ C_1 & D_1 \end{bmatrix} = \begin{bmatrix} 1 & 0 \\ -2/R_1 & 1 \end{bmatrix} \begin{bmatrix} 1 & L_1 \\ 0 & 1 \end{bmatrix} \begin{bmatrix} 1 & 0 \\ -1/f_1 & 1 \end{bmatrix} \begin{bmatrix} 1 & L_2 \\ 0 & 1 \end{bmatrix} \begin{bmatrix} 1 & L_2 \\ 0 & 1 \end{bmatrix} \begin{bmatrix} 1 & 0 \\ -1/f_1 & 1 \end{bmatrix} \begin{bmatrix} 1 & L_1 \\ 0 & 1 \end{bmatrix}, \quad (1)$$

$$\begin{bmatrix} A_2 & B_2 \\ C_2 & D_2 \end{bmatrix} = \begin{bmatrix} 1 & 0 \\ -2/R_2 & 1 \end{bmatrix} \begin{bmatrix} 1 & L_3 \\ 0 & 1 \end{bmatrix} \begin{bmatrix} 1 & 0 \\ -1/f_2 & 1 \end{bmatrix} \begin{bmatrix} 1 & L_4+L_5 \\ 0 & 1 \end{bmatrix} \begin{bmatrix} 1 & L_4+L_5 \\ 0 & 1 \end{bmatrix} \begin{bmatrix} 1 & 0 \\ -1/f_2 & 1 \end{bmatrix} \begin{bmatrix} 1 & L_3 \\ 0 & 1 \end{bmatrix}, \quad (2)$$

where R_1 and R_2 are the curvature radii of the mirrors M_1 and M_2, L_1-L_5 are the lengths defined in Fig. 2. Only when both 1064- and 1319-nm laser beams oscillate in the stable region simultaneously, the whole laser system can be regarded as a stable one, which is

$$|(A_i + D_i)/2| \le 1 (i = 1, 2). \quad (3)$$

By the above equations, a set of optimum parameters are picked out through calculation and simulation. When $L_1 = 7.1$ cm, $L_2 = 6.8$ cm, $L_3 = 6$ cm, $L_4 + L_5 = 8$ cm, and $R_1 = R_2 = 1$ m, the stability of the linear (for 1064 nm) and L-shaped (for 1319 nm) resonators is described in Fig. 3. It is shown that with

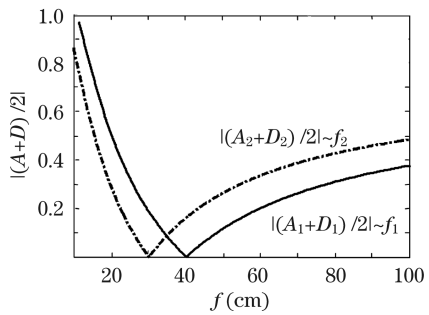

Fig. 3. Cavity stability condition $|(A+D)/2|$ as a function of thermal focal length f of the rod.

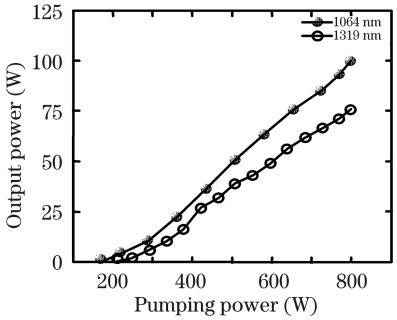

Fig. 4. Output power of fundamental beams.

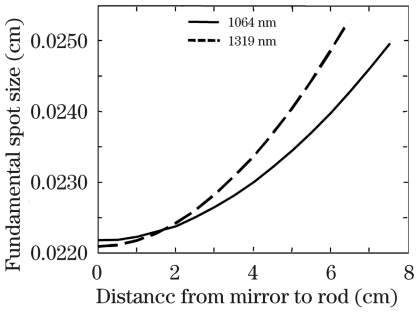

Fig. 5. Fundamental spot size distributions from the output mirror to the laser rods A and B.

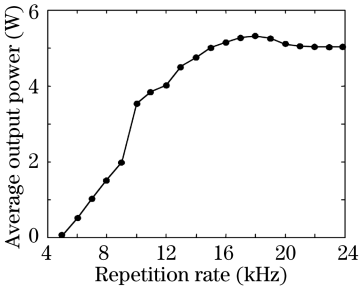

Fig. 6. 589-nm output power at different repetition rates of AOMs.

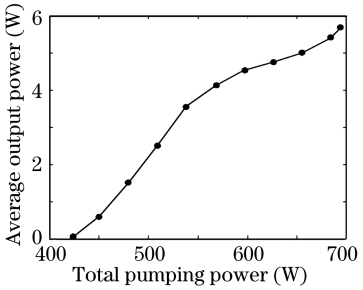

Fig. 7. 589-nm output power versus LD pumping power.

the variation of the thermal focal length from 100 to 10 cm, the whole laser system operates stably all the time, that is, it can present a wide enough thermal stable region for the two fundamental wavelength lasers and 589-nm yellow radiation.

In order to achieve high power sum-frequency generation, the power ratio of the 1064- and 1319-nm beams should be taken into account. According to the law of conservation of energy, one 1064-nm photon and one 1319-nm photon will produce one 589-nm photon. Therefore, it can be deduced that the optimum power ratio of the two fundamental beams is about 1.24:1. 1064- and 1319-nm laser beams oscillate in their own cavity, respectively. When the mirror M_3 is replaced with a flat output coupler (with the transmittance of 10% at 1064 nm), the 1064-nm beam oscillates between M_1 and M_3 with only Nd:YAG A working. Similarly, the mirror M_3 can also be replaced with another output coupler (with the transmittance of 10% at 1319 nm) and the 1319-nm beam oscillates in the L-shaped cavity with only Nd:YAG B working. The experimental results are shown in Fig. 4, from which we can choose proper power ratio of the two fundamental beams in the following experiment. When the powers of 1064- and 1319-nm lasers are given, the corresponding power of LDs will be determined[5]. In the experiment, the thermal focal lengths of Nd:YAG rods A and B are about 25 and 20 cm, respectively, when the corresponding diode pump powers are 385 and 310 W. Under this condition, the dual-wavelength fundamental spot size distributions from the mirror M_3 to the rods A and B are calculated and simulated, as shown in Fig. 5. It can be seen that the difference between the two fundamental spot sizes is small near the mirror M_3, especially within the distance of 2 cm. The high degree of spatial overlap between the two fundamental beams is beneficial

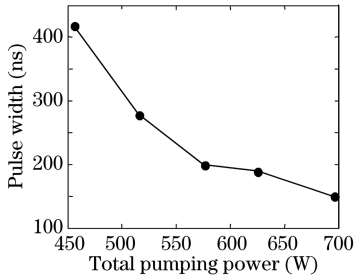

Fig. 8. Pulse width of 589-nm laser with the variation of pumping power.

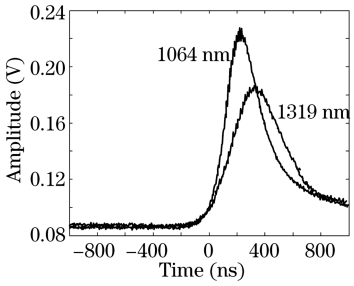

Fig. 9. Pulse widths of two fundamental beams.

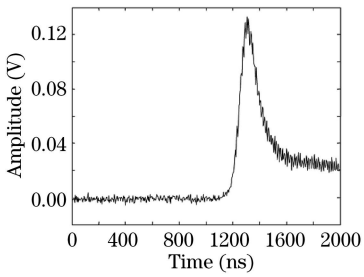

Fig. 10. Pulse width of 589-nm output laser.

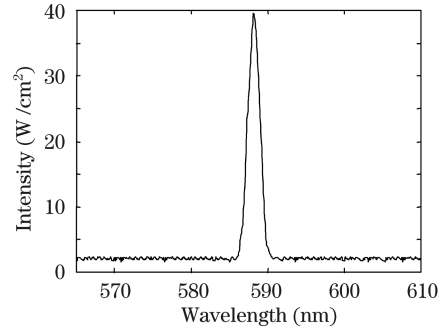

Fig. 11. Spectrum of 589-nm output laser.

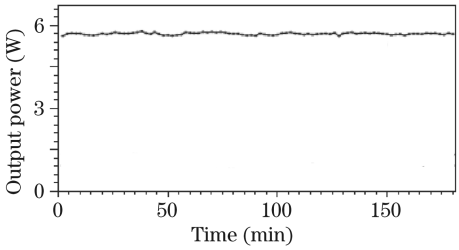

Fig. 12. Stability of 589-nm laser within three hours.

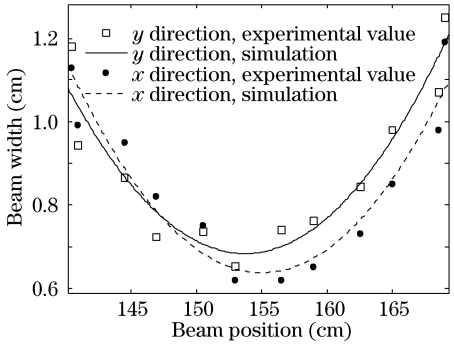

Fig. 13. Quality factors of 589-nm laser.

to increasing the frequency conversion efficiency.

In the experiment, the repetition rates of the two AOMs are the same all the time. We measured the output power of 589-nm yellow laser as a function of the repetition rates. Figure 6 shows the result. It can be seen that, as the repetition rate increases, there is an optimal value of 18 kHz corresponding to the maximum output power of the yellow laser. Furthermore, when the Q-switches work at the optimum repetition rate, the average output power of 589-nm laser as a function of diode pumping power is also recorded, as shown in Fig. 7. The yellow laser power increases nearly in proportion to the diode pumping power and finally reaches 5.7 W when the total LD pumping power is about 695 W. In addition, the measured pulse width of the 589-nm yellow laser drops with the total pump power increasing in the experiment (Fig. 8) and the pulse widths of 1064- and 1319-nm lasers are 280 and 390 ns, respectively (Fig. 9). It can be seen that spatial overlap of the two beams is not good enough to achieve high conversion efficiency, even though a digital delayed pulse generator is adopted. At the maximum output power, the corresponding optical-to-optical conversion efficiency from the two fundamental waves to the sum frequency generation is 15.2% and the pulse width of the yellow laser is 150 ns (Fig. 10) at the repetition rate of 18 kHz. We also measured the spectrum of the yellow laser (Fig. 11). The full-width at half-maximum (FWMH) is 1.94 nm and the central wavelength is at 588.15 nm, which indicates that there are high quality coatings on the mirrors. The instability of the yellow laser is less than 2% within 3 h (Fig. 12) and no damage to the KTP crystal is observed. Finally, the beam quality factors of the yellow laser were also measured, which are $M_x^2 = 4.96$, $M_y^2 = 5.08$ (Fig. 13).

In conclusion, a T-shaped thermal-insensitive cavity is designed to obtain a 589-nm yellow laser by intra-cavity sum-frequency mixing. In the experiment, a 5.7-W 589-nm laser is obtained when the total pumping power is 695 W, and the optical-to-optical conversion efficiency from the two fundamental waves to the sum frequency generation is 15.2%. At the maximum output power, the pulse width is 150 ns at the repetition rate of 18 kHz and the instability of the yellow laser is less than 2% within 3 h. The beam quality factors are $M_x^2 = 4.96$, $M_y^2 = 5.08$.

This work was supported by the National "863" Program of China (No. 2007AA03Z407) and the Northwest University Graduate Innovation and Creativity Funds (No. 08YZZ45).

References

1. X. Li, J. Shao, H. Zhang, and Y. Lu, Chinese J. Lasers (in Chinese) **35,** 206 (2008).
2. Y. Wan, K. Han, Y. Wang, and J. He, Chin. Opt. Lett. **6,** 124 (2008).
3. X. Liu, Z. Wang, Q. Wu, X. Yan, T. Liu, and T. Zuo, Chin. Opt. Lett. **5,** 409 (2007).
4. D. Chang, X. Liu, Y. Wang, Q. Ge, X. Jia, and K. Peng, Chinese J. Lasers (in Chinese) **35,** 323 (2008).
5. A. Geng, Y. Bo, X. Yang, H. Li, Z. Sun, Q. Peng, X. Wang, G. Wang, D. Cui, and Z. Xu, Opt. Commun. **255,** 248 (2005).
6. Y. Bo, A.-C. Geng, Y.-F. Lu, X.-D. Yang, Q.-J. Peng, Q.-J. Cui, D.-F. Cui, and Z.-Y. Xu, Chin. Phys. Lett. **23,** 1494 (2006).
7. X. Fu, H. Tan, Y. Li, E. Hao, and L. Qian, Chinese J. Lasers (in Chinese) **34,** 1043 (2007).
8. J. C. Bienfang, C. A. Denman, B. W. Grime, P. D. Hillman, G. T. Moore, and J. M. Telle, Opt. Lett. **28,** 2219 (2003).
9. J. D. Vance, C.-Y. She, and H. Moosmüller, Appl. Opt. **37,** 4891 (1998).
10. B. Wang, H. Tan, J. Peng, J. Miao, and L. Gao, Opt. Commun. **271,** 555 (2007).
11. M. B. Danailov and P. Apai, J. Appl. Phys. **75,** 8240 (1994).
12. G. A. Henderson, J. Appl. Phys. **68,** 5451 (1990).
13. T. H. Jeys, A. A. Brailove, and A. Mooradian, Appl. Opt. **28,** 2588 (1989).
14. C. A. Denman, J. D. Drummond, M. L. Eickhoff, R. Q. Fugate, P. D. Hillman, S. J. Novotny, and J. M. Telle, Proc. SPIE **6272,** 62721L (2006).
15. T. D. Kawahara, T. Kitahara, F. Kobayashi, J. Yamashita, Y. Satio, and A. Nomura, Proc. SPIE **4893,** 270 (2003).
16. S. Zhao, J. Yao, D. Xu, R. Zhou, B. Zhang, J. Zhou, and P. Wang, Proc. SPIE **5627,** 461 (2005).
17. Z. Feng, C. Li, X. Li, J. Wang, and J. Bai, Acta Opt. Sin. (in Chinese) **28,** 1543 (2004).
18. H. Wang, Z. Zhou, H. Cao, and W. Huang, J. Optoelectron. Laser (in Chinese) **14,** 149 (2003).